Envelope solitons and modulation instability of dipole-exchange magnetization waves in yttrium iron garnet films

B. A. Kalinikos, N. G. Kovshikov, and A. N. Slavin

V.I. Ulyanov (Lenin) Institute of Electrical Engineering, Leningrad
(Submitted 3 April 1987)
Zh. Eksp. Teor. Fiz. **94**, 159–176 (February 1988)

Microwave nonlinear dipole-exchange magnetization waves are studied experimentally in single-crystal films of yttrium iron garnet. Pulsed excitation and propagation of waves reveal formation of solitons of the envelope. These solitons form only within narrow frequency intervals located in the zones of strong dispersion near dipole "gaps" in the spectrum of spin waves in films with a limited surface spin mobility. Single-soliton and multisoliton propagation of magnetization waves is observed and the soliton parameters are determined. A study is made of a modulation instability which appears under conditions of monochromatic continuous excitation and of propagation of magnetization waves of finite amplitude within the same strong-dispersion intervals. A theoretical interpretation of the observed nonlinear phenomena is provided.

1. INTRODUCTION

Ideas from the modern theory of nonlinear waves have been recently adopted in the physics of magnetic phenomena. In many papers published in the last decade considerable progress has been made in theoretical studies of nonlinear magnetization waves in media which can be described by the Landau–Lifshitz equation (see, for example, Ref. 1–3 and the literature cited there). The appearance of new concepts such as those of a soliton or a strange attractor, has stimulated new experiments designed to study nonlinear wave processes in magnetic crystals.

In our view, among the most promising classes of materials for the investigation of spin wave processes are ferromagnetic films. The relative simplicity of the techniques for the excitation and detection of spin waves, the richness of their dispersion characteristics, the accessibility of waves from the surface of the film, and the weak attenuation per unit wavelength all make ferromagnetic films convenient objects for investigating spin wave processes themselves and for modeling wave equations in dispersive media in general.

Single-crystal yttrium iron garnet (YIG) films stand out from materials with the necessary homogeneity of properties and low magnetic losses. The room-temperature magnetic dissipation parameter of these films has an extremely low value ($\Delta H_k = 0.1$–0.3 Oe at microwave frequencies) so that it is easy to achieve directional propagation of microwave magnetization waves over distances of few or even few tens of millimeters (which amounts to hundreds and thousands of the wavelengths of a traveling wave). Moreover, the low magnetic losses and the readily attained high specific microwave powers in films when the absolute value of the power is still low make it easy to carry out nonlinear wave experiments. It is worth noting that the dispersion characteristics of the excited waves and, therefore, also the magnitude and sign of the nonlinearity of YIG films depend strongly on the magnitude and direction of the external static magnetic field, which makes it possible to vary these quantities within a wide range.

These properties of YIG films are some of the reasons why several interesting nonlinear phenomena have been discovered in these films, particularly parametric amplification of traveling waves,[4] formation of magnetic solitons,[5–7] modulation instability of magnetization waves,[8–10] transition of a modulation instability from a coherent to a stochastic regime, and the appearance of strange attractors.[11]

Our task was to investigate experimentally, the nonlinear properties of microwave magnetization waves of finite amplitude propagating under pulsed and continuous conditions in single-crystal YIG films, with the aim of demonstrating experimentally the existence of magnetization wave envelope solitons and of modulation instability of these waves.

2. DIPOLE-EXCHANGE SPECTRUM OF MAGNETIZATION WAVES IN A FERROMAGNETIC FILM

The experimental investigations reported below were based on specific ("film") properties of the dispersion of spin waves. We shall review these properties briefly by considering a transversely magnetized ferromagnetic film.

In allowing for the characteristic features of the spectrum of spin waves in a film the theoretical analysis should allow for the Zeeman, magnetic dipole–dipole, and exchange interactions and also for the characteristics of the state of surface spins (exchange boundary conditions). An analysis carried out subject to these provisos shows that the spin waves have discrete multiwave spectrum, and that each normal wave has its own distribution of variable magnetization across the ferromagnetic film thickness (see, for example, Refs. 12 and 13). The dispersion curves of all the normal waves propagating in the plane of the film begin at points corresponding to the frequencies of spin-wave resonance (SWR) modes. The exact dispersion law of dipole-exchange spin waves $\omega_n(\mathbf{k})$ is implicit. However, as shown in Ref. 13, the dispersion characteristics of waves in transversely magnetized films can be described using the following relationship obtained using perturbation theory:

$$\omega_n^2 = (\omega_H + \alpha\omega_M k_n^2)(\omega_H + \alpha\omega_M k_n^2 + \omega_M P_{nn}), \qquad (1)$$

where $\omega_H = \gamma H_i$; $\omega_M = \gamma 4\pi M_0$; γ is the modulus of the gyromagnetic ratio for the electron spin; H_i is the static internal magnetic field; $4\pi M_0$ is the equilibrium magnetization; α is the inhomogeneous exchange interaction constant; $k_n^2 = k^2 + \varkappa_n^2$; k is the wave number describing the wave process in the film plane and having a continuous set of values; $\varkappa_n = n\pi/L$ is the transverse wave number which assumes a

 0038-5646/88/020303-10$04.00

discrete series of values; n is the integral number of the wave mode; L is the ferromagnetic film thickness; and $P_{nn} = p_{nn'}$ $(n' = n)$ is a matrix element of the dipole–dipole interaction depending on the nature of the exchange boundary conditions. In the long-wavelength approximation corresponding to $kL < 1$ in the case of pinned surface spins the matrix element in question is

$$P_{nn'} = 2kL(2-kL)/\pi^2 nn', \quad n,\ n' = 1, 3, 5, \ldots, \tag{2}$$

$$P_{nn'} = 2(kL)^2/\pi^2 nn', \quad n,\ n' = 2, 4, 6, \ldots. \tag{3}$$

Both theoretical and experimental results show[14] that only the odd spin wave modes are excited effectively in films with pinned surface spins. The highest group velocity $v_{gn} = \partial\omega_n/\partial k$ is exhibited by the lowest wave mode with $n = 1$ at long wavelengths. It is physically clear that the fastest of the waves excited at the operating frequency determines the transfer of a microwave signal by the spin system of the film.

For example, the attenuation $\exp[i(\omega t - kx)]$ of a wave which has traveled a distance l is (in decibels)

$$A = 20 \lg[\exp(k''l)], \tag{4}$$

where k'' is the imaginary part of the wave number $k = k' - ik''$. In the approximation of weak dissipation, when $\omega'' < \omega'$ holds (ω' and ω'' are the real and imaginary components of the natural frequency of a spin wave), we can easily show that $k'' = \omega''(\partial\omega'/\partial k')^{-1}$. Therefore, the relationship (4) can be rewritten in the form

$$A \approx 20 \lg\left[\exp\left(\frac{\omega''}{v_g} l\right)\right] \approx 8.69 \frac{\omega''}{v_g} l, \tag{5}$$

which shows that a reduction in the group velocity increases the attenuation of the signal transferred by a spin wave.

An analysis of the spectrum of dipole-exchange spin waves shows that in the case of moderately thin films ($L > 0.2$ μm in the case of YIG films at frequencies in the 6-cm range of wavelengths) the dispersion curve of the lowest-order wave intersects the dispersion curves corresponding to other spin waves. At the points of intersection of the dispersion branches of Eq. (1) with numbers n and n' corresponding to waves of the same parity, the magnetic-dipole interaction results in hybridization and formation of dipole gaps in the spectrum. This effect is described approximately by the dispersion equation[12,13]

$$(\omega^2 - \omega_n^2)(\omega^2 - \omega_{n'}^2) = \omega_M^2 \Omega_{nk} \Omega_{n'k} P_{nn'}^2, \tag{6}$$

where $\Omega_{nk} = \omega_H + \omega_M \alpha k_n^2$.

The width of a dipole gap $\delta\omega$ at the point of intersection (ω_0, k_0) of the branches with numbers n and n' can be found from[13]

$$\delta\omega_{nn'} \approx \frac{\omega_M (\Omega_{nk}\Omega_{n'k})^{1/2}}{\omega_0} P_{nn'}. \tag{7}$$

A calculation based on Eq. (7) shows that in the case of films of micron thicknesses with free surface spins the dipole gaps are considerably smaller than the relaxation frequency $\omega_r = \gamma \Delta H_k$. However, in the case of films with pinned surface spins the gaps are considerably greater than the relaxation frequency and, consequently, they can be observed experimentally.

Figure 1a shows a dipole-exchange spectrum of odd (symmetric) spin waves in a transversely magnetized YIG film of thickness $L = 5.8$ μm ($\alpha = 3.1 \times 10^{-12}$ cm^{-2}, $\omega_M/2\pi = 4.9$ GHz, $\omega_H/2\pi = 4.312$ GHz) calculated from the dispersion equations (1) and (6) in the case of pinned surface spins. The dipole gaps in the spectrum form in the vicinity of the points of degeneracy of the fundamental mode ($n' = 1$) with higher modes characterized by odd numbers n. Near the gaps the group velocity changes rapidly as a result of a change in the frequency from a relatively large value corresponding to the fundamental mode ($n' = 1$) to a value which is approximately n^2 times smaller and which corresponds to a higher mode with a number n, i.e., the group velocity exhibits strong dispersion.

Figure 1b shows the frequency dependence of the group velocity $v_g(\omega)$ calculated from Eqs. (1) and (6) of the fastest waves within the selected frequency intervals. It follows from Eq. (5) that this curve describes also the frequency dependence of the wave attenuation as it propagates in a film. The inset in Fig. 1c shows the $\omega(k)$ and $v_g(\omega)$ curves on an enlarged scale in the vicinity of a gap characterized by $n' = 1$ and $n = 17$.

We conclude this discussion of the dispersion properties of spin waves by stressing once again that in the vicinity of the dipole gaps the spectrum of spin waves of films with pinned surface spins has pronounced frequency intervals of strong dispersion. It is in these intervals that the nonlinear phenomena described below are observed.

3. EXPERIMENTAL METHOD

Nonlinear magnetization waves were investigated using a prototype delay line (Fig. 2). This prototype consisted of

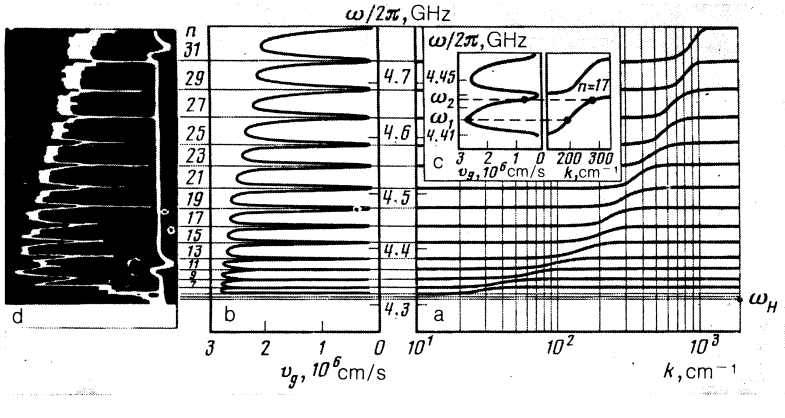

FIG. 1. Frequency spectrum (a, c) and group velocity (b, c) of magnetization waves in the investigated YIG film and the amplitude-frequency characteristic (d) of a prototype delay line recorded under linear conditions for $l = 4$ mm.

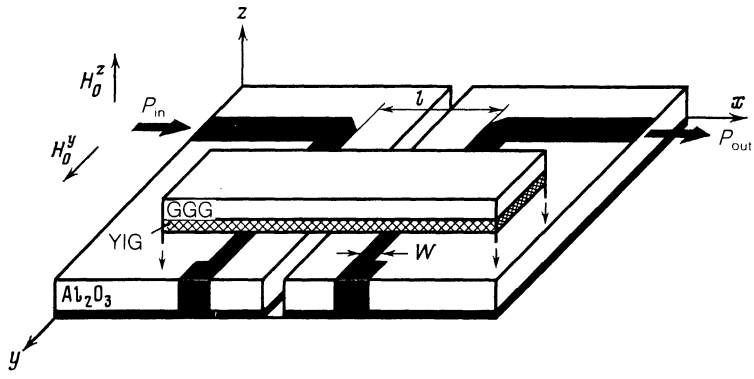

FIG. 2. Prototype delay line.

two Polikor plates on which transmitting and receiving spin-wave antennas of width $W = 30\,\mu$m and length up to 4 mm, together with microstrip supply lines, were formed by photolithography. These plates were attached to a metal base consisting of two movable halves which made it possible to vary continuously the distance between the transmitting and receiving antennas from 3 to 10 mm. A film sample was placed on top of the antennas and kept in place by a pressure device. The delay line was placed inside a gap of a permanent magnet which generated a magnetic field of the required intensity and direction. Measurements were made at room temperature under pulsed and continuous conditions.

In the pulsed case a microwave signal, reaching the transmitting antenna of the delay line from a klystron oscillator via a microwave amplifier, was used to excite magnetization waves. The maximum signal power beyond the amplifier could reach 1 W. The profile of the input microwave signal was monitored by deflecting part of it, identifying it, and applying it to one of the inputs of a dual-trace oscilloscope of the S1-74 type. The output microwave signal transmitted by the ferromagnetic film and recorded using the receiving antenna of the delay line was also rectified and applied to the other input of the oscilloscope.

The microwave spectrum of the signals at the input and output of the delay line was recorded using an S4-27 spectrum analyzer. The power of the input and output microwave signals was measured with an M3-21A thermistor power meter to within 20%. The frequency measurements were made employing a Ch3-34 electronic digital voltmeter.

In the pulsed excitation regime the microwave signal supplied by the klystron oscillator reached the microwave amplifier after passing first through a modulator. Modulation was imposed by pulses of 0.1–5 μs duration and a repetition frequency 10^2–10^5 Hz, supplied by a generator of rectangular pulses. The delay of a microwave rf pulse and the reduction of its amplitude during the propagation in the ferromagnetic film between the transmitting and receiving antennas of the delay line were displayed on the oscilloscope screen.

The investigated samples were single-crystal YIG films of thickness $L = 3$–8 μm characterized by low magnetic losses (dissipation parameter $\Delta H_k = 0.2$–0.3 Oe). These films were grown on gadolinium gallium garnet (GGG) substrates with (111) orientation by the method of liquid phase epitaxy. The film selected for our experiments exhibited characteristic signs of pinned surface spins. The criterion for judging the state of surface spins was the amplitude-frequency characteristic of a film, i.e., the frequency dependence of the attenuation of the microwave signal transmitted by the film. This characteristic was investigated using standard meters (of the R2-58 type with a Ya2R-67 detector) when the incident power was less that 10 μW, which ensured that the measurements were carried out under linear conditions.

We shall now consider the method used in the selection of films in greater detail. According to the theoretical ideas, the amplitude-frequency characteristic of a film with pinned surface spins should have characteristic dips in the frequency intervals of the dipole gaps in the spectrum. However, in the case of free surface spins, with $\delta\omega_{nn'} \ll \omega_r$, this characteristic should be smooth. These theoretical predictions were confirmed experimentally. Figure 3 shows a typical oscillogram of an amplitude-frequency characteristic obtained for a single-crystal YIG film of thickness $L \approx 5$ μm with free surface spins. Figure 1d shows the corresponding characteristic of a transversely magnetized YIG film ($L = 5.8$ μm, $\Delta H_k = 0.2$ Oe) selected for further experiments. The very good agreement between the frequency positions of the dipole gaps found by calculation (Fig. 1b) and experimentally (Fig. 1d), and also excitation of just the symmetric waves allowed us to assume that surface spins were pinned in the sample quite strongly. In practice we frequently encountered films exhibiting a "mixed" state of surface spins and it was found that the surface anisotropy varied from one film surface to another. A numerical analysis of the amplitude-frequency characteristics based on the theory of excitation of

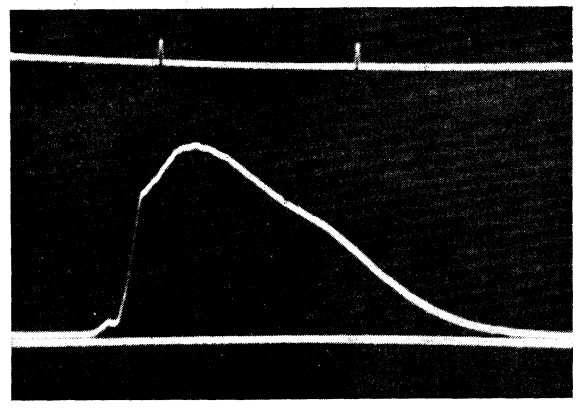

FIG. 3. Amplitude-frequency characteristic of a YIG film with free surface spins.

spin waves made it possible to determine the pinning parameters of surface spins on both faces of the film. A more detailed discussion of this topic is outside the scope of the present paper.

4. EXPERIMENTAL RESULTS

4.1. Pulsed regime

The first series of experiments carried out in the pulsed regime was made on a transversely magnetized (to saturation) YIG film of thickness $L = 5.8\ \mu$m when the distance between the antennas was $l = 4$ mm. The static internal magnetization field was $H_i = 1540$ Oe. The amplitude-frequency characteristic of this film is shown in Fig. 1d.

These measurements were carried out as follows. The transmitting antenna of the delay line was subjected to rf pulses of $\tau = 180$ ns duration at a carrier frequency selected to be in the vicinity of the $n' = 1$, $n = 17$ dipole gap in the spectrum of spin waves of this film (Fig. 1c). The power of the input rf pulses was varied within the range $P_{in} = 0.05$–50 mW.[1)]

The results of the first series of the experiments under pulsed conditions are presented in Figs. 4a–4i. The upper traces in the oscillograms in Figs. 4a–4i show the position of the input signal of the time scale and the lower traces demonstrate the shape of the envelope and the position of the output spin wave pulses. (It should be pointed out that amplification in the channels of a dual-trace oscilloscope, used to record the oscillograms in Figs. 4a–4i, was selected to be stronger for the lower trace than for the upper one.) Figure 4j shows, on an enlarged scale, a part of the amplitude-frequency characteristic of this film showing a dip corresponding to the $n' = 1$, $n = 17$ gap; the letters a–i identify the points at which the various oscillograms were recorded. The first three oscillograms (Figs. 4a–4c) were obtained by successively increasing in the carrier frequency ω from ω_1 to ω_2 (Fig. 1c), keeping constant the input power $P_{in} = 0.05$ mW, which was known to ensure linear propagation of spin waves. Clearly, at the frequency $\omega = \omega_1$ located between the gaps in the region of relatively weak dispersion it was found that the usual delayed pulse appeared at the exit from the ferromagnetic field (Fig. 4a); the profile and duration of this pulse differed little from the pulse applied to the input of the system. When the carrier frequency was shifted to a region of strong dispersion, corresponding to the edge of a gap, the profile and amplitude of such a pulse changed considerably because of the dispersion spreading (Fig. 4b), and at the point $\omega = \omega_2$, located several megahertz below the middle of the gap, it was found that the amplitude of the signal obtained from the ferromagnetic film was low and practically completely flattened by dispersion (Fig. 4c).

The oscillograms shown in Figs. 4c–4f were obtained for a fixed value of the carrier frequency $\omega = \omega_2$, but a gradually increasing input power P_{in}. Clearly, at some value of the input power ($P_{in} = 20$ mW) the "bunching" effect of the nonlinearity of the spin system compensated for the dispersion spreading and instead of the dispersion-smeared output pulse we observed a narrow peak representing a soliton of the spin wave envelope (Figs. 4e and 4f). The threshold for the appearance of a soliton in our experiments was $P_{in} = 10$–12 mW. The resultant envelope soliton lasted a time $\tau_s = 100$–120 ns, shorter than the duration of the input pulse $\tau = 180$ ns (Fig. 4f).

It should be pointed out that we observed the formation of solitons only in the region corresponding to the left edge of the gap, where $\partial^2\omega/\partial k^2 < 0$. In the region of the right-hand edge of the gap, where $\partial^2\omega/\partial k^2 > 0$, the dispersion spreading was not balanced by nonlinear bunching for the same input power $P_{in} = 20$ mW, and envelope solitons were not formed (Figs. 4g–4i).

These experiments allowed us to determine the velocity of a single envelope soliton v_s from its delay relative to the input pulse (Figs. 4c–4f). An increase in P_{in} resulted in a slow increase in the soliton velocity and at $P_{in} = 20$ mW the soliton velocity was $v_s = 2\times10^6$ cm/s. Within the limits of the experimental error, this soliton velocity was equal to the linear group velocity of spin waves at the frequency $\omega = \omega_2$.

A second series of experiments under pulsed conditions was made in the case of tangential magnetization of a ferro-

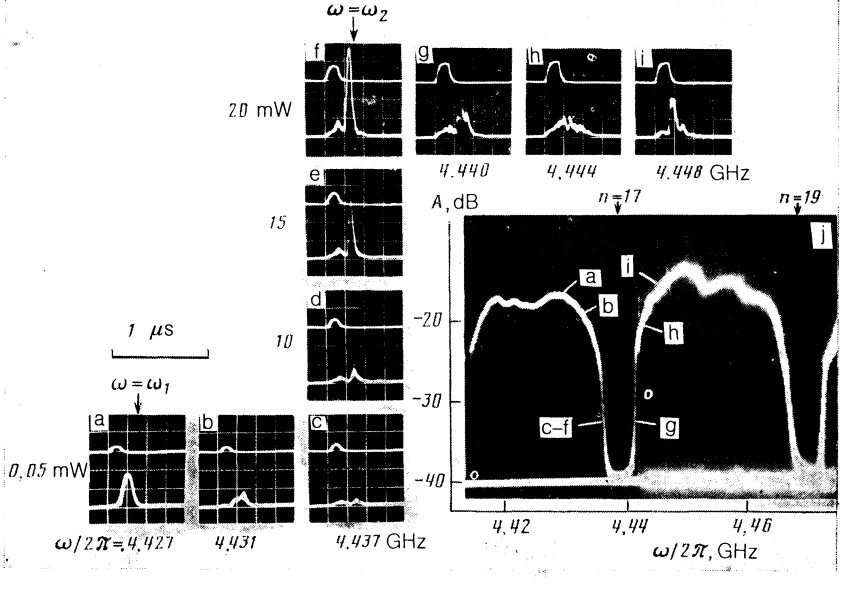

FIG. 4. a)–i) Oscillograms of the envelope of a pulse signal at the input (upper traces) and at the output (lower traces) of a prototype delay line obtained in the vicinity of a $n' = 1$, $n = 17$ dipole gap for different values of the input power P_{in} at different carrier frequencies ω. j) part of the amplitude-frequency characteristic of the prototype recorded under linear conditions in the vicinity of the $n' = 1$, $n = 17$ gap.

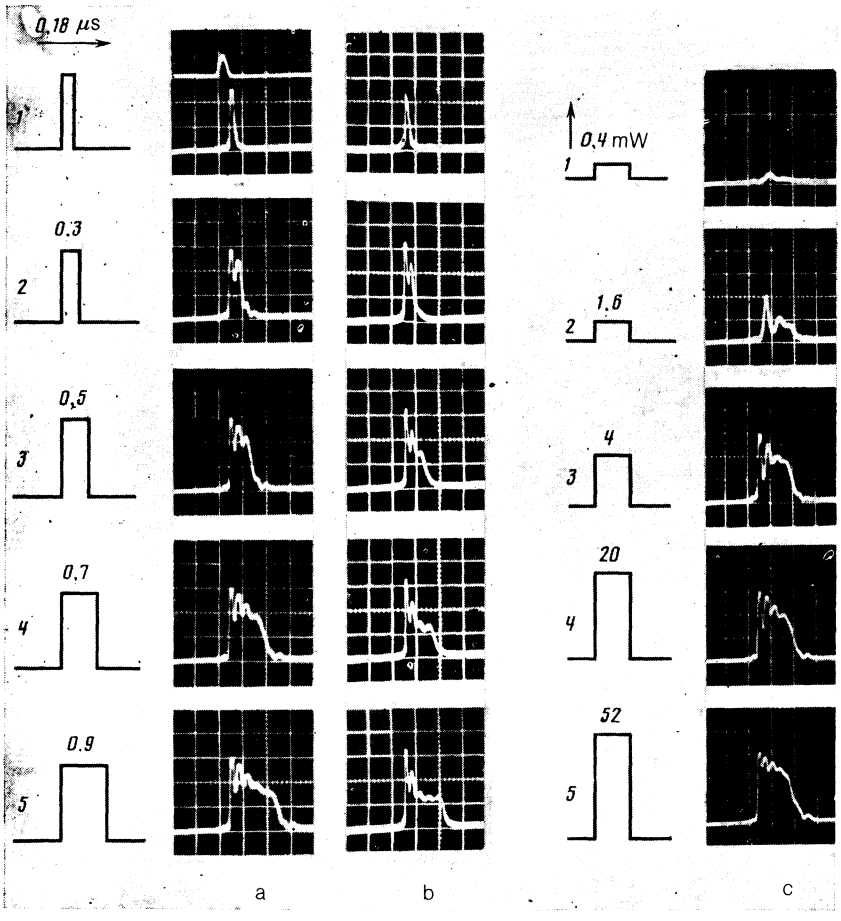

FIG. 5. Oscillograms of the envelope of a pulse signal at the output of the prototype delay line obtained for the carrier frequency corresponding to the point c in Fig. 4j. The series of oscillograms shown above were recorded for the following parameters: a) $P_{in} = 20$ mW, $l = 4$ mm, $\tau = 0.18$–0.9 μs; b) $P_{in} = 20$ mW, $l = 7$ mm, $\tau = 0.18$–0.9 μs; c) $P_{in} = 0.4$–52 mW, $l = 4$ mm, $\tau = 0.7$ μs.

magnetic field when a static magnetic field was directed along the transmitting and receiving antennas, and quasisurface spin waves were excited.[6,15] In this case we again observed envelope solitons. However, it should be stressed that, in contrast to the case of transverse magnetization of a film, soliton formation in the tangentially magnetized film occurred in the regions of strong dispersion located at frequencies above the dipole gaps in the spin wave spectrum, where $\partial^2\omega/\partial k^2 > 0$ held.

The purpose of the third series of experiments under pulsed conditions was to study the behavior of envelope solitons when the duration τ and power P_{in} of an input signal were increased.[7] In these measurements we again used a transversely magnetized YIG film of thickness $L = 5.8$ μm, but the internal magnetic field was now $H_i = 1190$ Oe. The carrier frequency $\omega/2\pi = 3453$ MHz was selected to be 3 MHz less than the midpoint of the $n' = i$, $n = 17$ dipole gap, which corresponded to the point $\omega = \omega_2$ in Fig. 1c. The left-hand edge of this gap corresponded to 3448 MHz and the right-hand edge to 3464 MHz.

The experimental results obtained are plotted in Fig. 5. The series of oscillograms denoted by a and b in Fig. 5 were recorded with the antennas separated by $l = 4$ and 7 mm, respectively. They demonstrated the profile of the envelope of a pulse signal leaving the selected ferromagnetic film when the input of the system was subjected to a rectangular pulse of fixed power $P_{in} = 20$ mW but of variable duration τ which was increased in steps from 180 to 900 ns. The upper curve in Fig. 5a(1) represents the position of the input pulse of length $\tau = 180$ ns. One soliton of $\tau_s = 120$ ns duration formed when the input pulse duration was $\tau = 180$ ns. An increase in the duration of the input pulse increased the number of solitons [Fig. 5a(2)–(4)] and for $\tau = 900$ ns we observed five envelope solitons of different amplitudes Fig. 5a(5)], i.e., multisoliton propagation of spin waves was observed.

A comparison of Figs. 5a and 5b demonstrated that an increase in the distance l traversed by a spin wave pulse did not alter significantly its envelope (as judged by the number and shape of the resultant solitons), but the delay time of solitons increased in proportion to the distance. The relative positions of solitons of different amplitudes were also practically unaffected [compare, for example, Fig. 5a(3) with Fig. 5b(3)]. This was evidence that the envelope velocity did not depend on the amplitude. The measured values of the velocity of single solitons in the case of multisoliton propagation were equal to within an experimental error, which amounted to 10%.

The next series of experiments (Fig. 5c) demonstrated evolution of a rectangular input pulse of $\tau = 700$ ns duration with a carrier frequency $\omega/2\pi = \omega_2/2\pi = 3453$ MHz when the distance between the antennas was $l = 4$ mm and the input power P_{in} was increased from 0.4 to 52 mW. When P_{in} was increased, the number of envelope solitons formed in the ferromagnetic film increased from 1 to 4.

We observed similar effects in normally magnetized YIG films of thickness from 3 to 7 μm near the majority of the dipole gaps in the spin wave spectrum when the distance

between the transmitting and receiving antennas was $l = 4$–10 mm.

4.2. Continuous regime

In the case of continuous excitation we studied propagation of a dipole-exchange spin wave of finite amplitude with its frequency lying in the vicinity of one of the dipole gaps of a transversely magnetized YIG film.[8] The aim of the measurements carried out in the continuous regime was to determine whether an unmodulated traveling spin wave with frequency lying in the parts of the spectrum where envelope solitons were observed in the pulse regime became unstable under modulation when the amplitude was increased.

The results of the measurements are presented in Fig. 6. This figure gives the frequency spectra 1–8 and the corresponding oscillograms of the envelope of a microwave signal emerging from a ferromagnetic film, which were obtained as the input P_{in} of an unmodulated input signal gradually increased. The lower traces in the oscillograms 1–8 correspond to the zero level of the video signal. Oscillograms and spectrograms in Fig. 6 were obtained for a YIG film of thickness $L = 5.8$ μm when the distance between the antenna was $l = 4$ mm. The input signal frequency was $\omega_c/2\pi = 3453$ MHz; it was selected to be the same as the frequency at which envelope solitons form in the pulsed regime (Fig. 5).

The first pair of photographs in Fig. 6(1) was obtained under conditions of linear propagation of spin waves when the receiving antenna detected a wave of constant amplitude. When the power of the input unmodulated signal increased to $P_{in} = 12$ mW a spin wave of constant amplitude became unstable during its propagation in the ferromagnetic film. The receiving antenna then recorded a modulated spin wave with an asymmetric frequency spectrum in which the amplitude of the low-frequency side components was considerably greater than the amplitude of the high-frequency side components, and the modulation frequency was $f_m = 4$–6 MHz [Fig. 6(2)].

A further increase in P_{in} increased both the modulation frequency M and the modulation frequency f_m of the spin wave at the exit from the ferromagnetic film [Figs. 6(3) and 6(4)], and at $P_{in} = 20$ mW there was an abrupt change from a regime characterized by the modulation coefficient $M < 1$ [Fig. 6(4)] to an "over modulation" regime with $M > 1$ [Fig. 6(5)]. In the latter regime the minima of the signal envelope at the exit of the ferromagnetic film reached zero level and the energy concentrated in the low-frequency side band of the signal spectrum exceeded the energy at the fundamental frequency [Fig. 6(5)]. A further increase in P_{in} again resulted in an abrupt change to the regime with $M < 1$ [Fig. 6(6)]. Then at $P_{in} = 30$ mW the modulation coefficient M decreased, the frequency spectrum of the modulation instability became wider and continuous, and the profile of the envelope of the output signal exhibited strong noise distortions [Fig. 6(7)]. Finally, at $P_{in} = 40$ mW [Fig. 6(8)] coherent modulation of spin waves at the exit from the investigated ferromagnetic film practically disappeared and the output signal was found to be stochastically modulated. The spectrum of modulation of spin waves then merged into a single noise peak and the average frequency of this stochastic modulation decreased. The profile of the envelope of the output signal also became noise-like [Fig. 6(8)].[2)]

In comparing Figs. 6(1)–(8) we should bear in mind that the sensitivity of the instruments used in our apparatus decreased in inverse proportion to P_{in}, so that in Fig. 6(8) the amplitude scale was four times greater than in Fig. 6(1).

These experiments established that an increase in the input signal power P_{in} first induced a modulation instability in narrow frequency intervals of strong dispersion below the dipole gaps where $\partial^2\omega/\partial k^2 < 0$ (Fig. 6). As the input power was increased, the frequency intervals of existence of this modulation instability became wider, extending to regions of strong dispersion above the gaps where $\partial^2\omega/\partial k^2 > 0$, as well as to regions between the dipole gaps. Therefore, it was found that finite-amplitude spin waves gradually became modulation-unstable throughout the full frequency range of

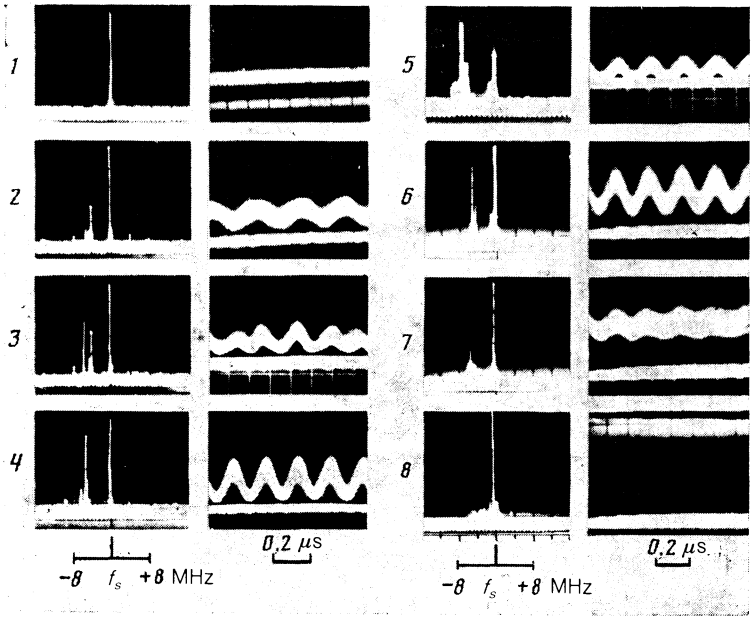

FIG. 6. Spectrograms and oscillograms of a continuous signal at the output of the prototype delay line obtained for input signal frequencies corresponding to the point c in Fig. 4j, using different input powers P_{in} (mW): 1) 10; 2) 12; 3) 16; 4) 18; 5) 20; 6) 22; 7) 30; 8) 40.

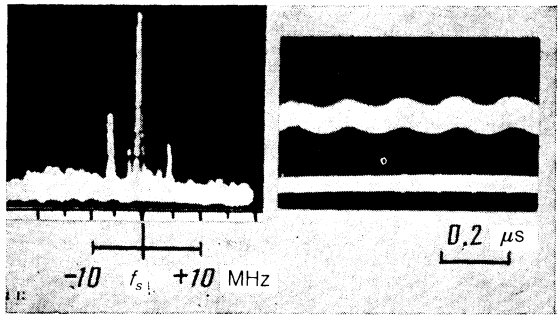

FIG. 7. Spectrograms and oscillograms of a continuous signal at the output of the prototype delay line obtained for an input signal frequency corresponding to the point g in Fig. 4j using an input power $P_{in} = 25$ mW.

their excitation. In the frequency intervals above the gaps and between the gaps it was found that, in contrast to the frequency below the gaps where $\partial^2\omega/\partial k^2 < 0$, the modulation instability spectrum contained as a rule both lower and upper side components and the depth of modulation remained low, $M < 0.3$ (Fig. 7). As P_{in} increased the modulation instability spectrum also became stochastic in these frequency intervals.

The modulation instability of finite-amplitude spin waves (with a modulation frequency f_m on the order of several megahertz) was recorded for all our YIG films with the pinned surface spins and with thicknesses from 3 to 7 μm.

It should be stressed once again that the modulation instability observed in frequency intervals of strong negative dispersion below the gaps, where in the pulsed regime we observed formation of envelope solitons, exhibited characteristic features of the minimum excitation threshold, asymmetric (single-band) frequency spectrum, and large modulation depth.

5. DISCUSSION OF EXPERIMENTAL RESULTS

The frequency of excitation ω of magnetization waves in the above experiments was selected so that three-wave first-order decay processes were impossible. The dominant role in the nonlinearity of magnetization waves was then played by four-wave processes of the type

$$\begin{aligned}\omega_{\mathbf{k}}+\omega_{\mathbf{k}_1}&=\omega_{\mathbf{k}_2}+\omega_{\mathbf{k}_3},\\ \mathbf{k}+\mathbf{k}_1&=\mathbf{k}_2+\mathbf{k}_3.\end{aligned} \tag{8}$$

Among the processes described by the system (8), we can distinguish the interaction of unidirectional waves

$$2\omega_{k_0}=\omega_{k_0+\varkappa}+\omega_{k_0-\varkappa}, \tag{9}$$

which in the $\varkappa \ll k_0$ case describe a modulational instability, whereas for $\varkappa \sim k_0$ they describe a decay instability, and also the processes of interaction of pairs of oppositely directed waves:

$$\omega_{k_0}+\omega_{-k_0}=\omega_{k_0\pm\varkappa}+\omega_{-(k_0\pm\varkappa)}. \tag{10}$$

Under our experimental conditions the processes described by Eq. (10) could contribute only in the near-field zone of the transmitting antenna.

Nonlinear properties of traveling magnetization waves will be described using the approach developed in Ref. 16. In this approach the dispersion equation (6), where the dependence on the wave amplitude is introduced in the familiar wave[17,18] and an allowance is made for magnetic dissipation, is related to a nonlinear evolution equation for the complex dimensionless amplitude φ of the envelope of a magnetization wave Ψ:

$$i\left(\frac{\partial\varphi}{\partial t}+\frac{\partial\omega}{\partial k}\frac{\partial\varphi}{\partial x}\right)+\frac{1}{2}\frac{\partial^2\omega}{\partial k^2}\frac{\partial^2\varphi}{\partial x^2}-\frac{\partial\omega}{\partial|\varphi|^2}|\varphi|^2\varphi=-i\omega_r\varphi, \tag{11}$$

where

$$\Psi(x,t)=\varphi(x,t)\exp[i(\omega_0 t-k_0 x)], \quad \Psi^2=m^2/2(4\pi M_0)^2,$$

m is the alternating magnetization, and ω_0 and k_0 are the frequency and wave vector of a magnetization wave.

It is shown in Ref. 19 that an evolution equation analogous to Eq. (11) is obtained for magnetization waves in a ferromagnetic film using the classical Hamiltonian formalism[20–22] if the four-wave interaction Hamiltonian of Eq. (8) is reduced only to the processes described by Eq. (9) which are characterized by $\varkappa \ll k_0$ and if it is assumed that all the interacting waves belong to the same dispersion branch (i.e., that they are characterized by the same distribution of the alternating magnetization across the film thickness).

In the specific case in which there are no losses $\omega_r = 0$, Eq. (11) reduces to the classical nonlinear Schrödinger equation, the solutions of which have been investigated quite thoroughly.[16,23] The simplest solutions of the nonlinear Schrödinger equation are steady-state envelope waves (see p. 135 in Ref. 16). These solutions are bounded in the limit $\varphi \to 0$ and are of the form

$$\varphi(x,t)=a(\xi)\exp\left(-ia_0^2\frac{\partial\omega}{\partial|\varphi|^2}t\right), \tag{12}$$

where $a(\xi)$ is the real amplitude of the envelope of a magnetization wave; $\xi = x - v_g t$; a_0 is a constant representing the average amplitude of the envelope. Three types of solution are possible for $a(\xi)$: an aperiodic solution corresponding to an isolated wave of the soliton type see [Eq. (28.12) in Ref. 16] and two periodic solutions corresponding to modulated waves for which the envelope does not reach zero level [Eq. (28.13) in Ref. 16] and intersects the zero level [Eq. (28.15) in Ref. 16]. These solutions for steady-state envelope waves and the more general soliton solutions of the nonlinear Schrodinger equation described in Ref. 23 can exist if the condition of instability $a(\xi) = a_0$ of a constant-amplitude wave against longitudinal perturbations (modulation instability condition or the Lighthill criterion) is satisfied:

$$\frac{\partial\omega}{\partial|\varphi|^2}\Big/\frac{\partial^2\omega}{\partial k^2}<0. \tag{13}$$

Self-modulation of a finite-amplitude wave a_0 in a nonlinear medium with dispersion, described by Eqs. (28.12)–(28.18) in Ref. 16, appears because a parametric instability of Eq. (9) develops as the wave propagates, and the maximum growth rate β is

$$\beta=a_0^2\frac{\partial\omega}{\partial|\varphi|^2} \quad \text{for} \quad \varkappa_0=\left(2|\beta|\Big/\left|\frac{\partial^2\omega}{\partial k^2}\right|\right)^{1/2}, \tag{14}$$

where $\varkappa_0$ is the wave number of the resultant modulation.

In real media which are characterized by dissipation

and for which the parametric process of Eq. (9) has a threshold, the inequality of Eq. (13) is not a sufficient condition for the appearance of a modulation instability and for the formation of envelope solitons. In fact, a modulation instability can appear in a medium with dissipation if the influence of dispersion (and of the competing nonlinearity) on the profile of the propagating wave considerably exceeds the influence of dissipation, i.e., if dissipation is a small perturbation in Eq. (11):

$$\omega_r \ll a_0^2 \left| \frac{\partial \omega}{\partial |\varphi|^2} \right|, \tag{15a}$$

$$\omega_r \ll \left(\frac{2\pi}{\tau v_g} \right)^2 \left| \frac{\partial^2 \omega}{\partial k^2} \right|, \tag{15b}$$

where τ is the characteristic time scale of the envelope wave (for example, duration of an input wave pulse). It should be noted that if the inequality of Eq. (15a) is transformed into the corresponding equality, we obtain the following condition for the parametric threshold of the process described by Eq. (9) (Refs. 20 and 24):

$$a_0^2 = \omega_r \Big/ \left| \frac{\partial \omega}{\partial |\varphi|^2} \right|.$$

In addition to satisfying the conditions of Eq. (15), it is essential to ensure that the parametric instability of Eq. (9) develops during the time required for a wave to propagate from the transmitting to the receiving antenna, i.e., we must satisfy also the condition

$$l \gg v_g \Big/ \left(\left| \frac{\partial \omega}{\partial |\varphi|^2} \right| a_0^2 - \omega_r \right), \tag{16}$$

where l is the distance between the transmitting and receiving antennas. We must point out that the condition (16) is independent of the duration τ of the input pulse. Therefore, in the pulsed regime, modulational instability and formation of envelope solitons may be observed also when the input pulse "does not fit" between the antennas, i.e., when $l < \tau v_g$.

Formation of N envelope solitons from a rectangular input pulse of finite duration τ occurs also provided the amplitude a_0 of the input pulse exceeds a certain critical amplitude governed by the condition[23,18]:

$$a_0^2 > \frac{(2N-1)^2}{16} \left(\frac{2\pi}{\tau v_g} \right)^2 \left| \frac{\partial^2 \omega}{\partial k^2} \right| \Big/ \left| \frac{\partial \omega}{\partial |\varphi|^2} \right|, \tag{17}$$

where $N = 1, 2, 3, \ldots$.

It was shown in Ref. 25 that when the conditions (15) and (16) are satisfied, the presence of weak attenuation $\omega_r \neq 0$ in Eq. (11) does not result in qualitative changes in steady-state solutions of the nonlinear Schrödinger equation, and nonlinear excitations described by these solutions are quite stable and long-lived also in the case of a lossy medium.

We shall now use Eqs. (13)–(17) to obtain numerical estimates for the experimental situation described above. The coefficient $\partial\omega/\partial|\varphi|^2$ representing the nonlinearity can be found from the dispersion equation (6) and it amounts to

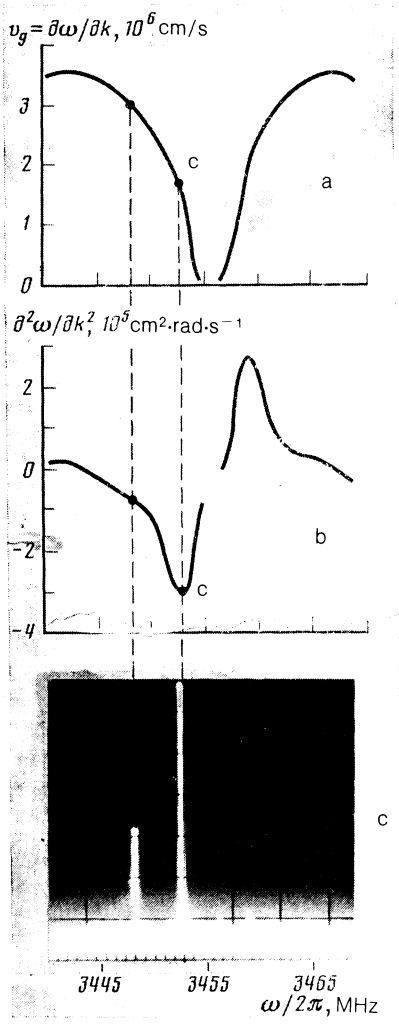

FIG. 8. Frequency dependence of the group velocity (a) and of the dispersion parameter (b) obtained in the vicinity of an $n' = 1$, $n = 17$ dipole gap. c) Spectrogram of a continuous signal at the output of the prototype delay line obtained for an input power $P_{in} = 12$ mW.

$\partial\omega/\partial|\varphi|^2 \approx \omega_m = 3.10^{10}$ rad/s. The relaxation frequency of the investigated film is $\omega_r = 6\times10^6$ rad/s. The spectral derivatives $\partial\omega/\partial k = v_g$ and $\partial^2\omega/\partial k^2$ can be found from the experimental curve in Fig. 4j using Eq. (5). The dependences $v_g(\omega)$ and $\partial^2\omega/\partial k^2$ obtained in this way near the $n' = 1$, $n = 17$ gap are plotted in Figs. 8a and 8b. The bulk of our experiments on a transversely magnetized film were carried out using a carrier frequency ω close to the point of maximum dispersion (point c in Fig. 4j and in Figs. 8a and 8b). At this point the necessary condition for a modulational instabilty [Eq. (13)] is satisfied and the values of the spectral derivatives are $v_g = 1.8\times10^6$ cm/s and $\partial^2\omega/\partial k^2 = -3\times10^5$ cm^2·rad·s^{-1}.[3)] Using the theory of the excitation of spin waves in a ferromagnetic field,[12,14] we can calculate the amplitude P_{in} of a magnetization wave excited in the investigated film by a signal of power P_{in} applied to the input antenna. At the point c in Figs. 8a and 8b we find that in the case of our prototype delay line ($W = 30\,\mu$m, $L = 5.8\,\mu$m, $4\pi M_0 = 1750$ Oe) when the input power is $P_{in} = 20$ mW, the wave amplitude is $a_0 = 4\times10^{-2}$ (the amplitude m of the alternating magnetization is approximately 100 Oe). It then follows from Eqs. (14) and (15a) that the maximum parametric growth rate of the instability of Eq. (9) at the point c

is four times greater than the relaxation frequency ω_r. It follows from the criterion (16) that the distance between the antennas l necessary for the development of the instability is $l = 0.4$ mm, which is an order of magnitude less than the minimum distance between the antennas in the delay line ($l = 4$ mm). Therefore, all the conditions for the observation of a modulation instability and the formation solitons of the envelope or magnetization waves are satisfied at the point c.

The frequency of the modulational instability with the maximum growth rate is [for $\varkappa_0$ defined by Eq. (14)]

$$f_m = v_g \varkappa_0 / 2\pi = 5.1 \text{ MHz}.$$

It is clear from Fig. 6 that this value is very close to the modulation frequency found experimentally: 4–6 MHz.

The duration of a single envelope soliton, measured at half maximum for the values of v_g, $\partial^2\omega/\partial k^2$, $\partial\omega/\partial|\varphi|^2$, and a_0 found in our study can be estimated theoretically with the aid of Eq. (28.12) from Ref. 16 to be $\tau_s = 116$ ns. The soliton duration found experimentally is $\tau_s^{\text{exp}} = 120 \pm 20$ ns (Fig. 4). It also follows from Figs. 4–6 that all three types of steady-state nonlinear envelope waves described by Eqs. (28.13)–(28.15) of Ref. 16 are observed: isolated waves of the soliton type (Fig. 4f), a modulated wave with an envelope that does not reach zero level [Figs. 6(4) and 6(6)], and a modulation wave with an envelope intersecting the zero level [Fig. 6(5)].

The conditions of Eqs. (15b) and (17) make it possible to find the limits of the duration τ of an input pulse within which we can observe formation of envelope solitons, bearing in mind that the minimum value of the duration is limited by the condition for the existence of the minimum amplitude of a single soliton, Eq. (17), and the maximum duration is limited by the attenuation condition:

$$70 \text{ ns} < \tau < 780 \text{ ns}.$$

This estimate is confirmed by the experimental results. In particular, beginning from $\tau \approx 150$ ns a reduction in the duration of the input pulse begins to reduce the soliton amplitude, whereas at $\tau \approx 80$ ns the soliton disappears completely. In the case of longer input pulses ($\tau = 900$ ns) the attenuation smears out the soliton formation pattern and single solitons become difficult to distinguish near the trailing edge of a pulse [see Fig. 5a(5)]. Equation (17) can be used to calculate the number N of solitons formed from an input pulse of a given duration τ. The results of such a calculation are presented in Fig. 9. We can see that in the case of short input pulses the theory agrees well with the experimental results, but in the range $\tau > 600$ ns there are discrepancies. In our opinion these are due to the influence of attenuation.

Naturally, these discussions and estimates can be regarded only as a qualitative confirmation of the soliton nature of the observed effects than as a theory providing a quantitative description. The considerable difference between the experimental situation discussed by us and the classical model of Refs. 16, 20, and 23 is that in the vicinity of the dipole gaps the dispersion coefficients v_g and $\partial^2\omega/\partial k^2$ vary rapidly in magnitude and sign when the carrier frequency is varied, even within the limits of the spectrum of the envelope of the input signal (see Figs. 8a and 8b).

Moreover, an increase in the output power not only produces a parallel shift of the spectrum, associated with the nonlinear term in Eq. (11), but also induces deformation of the spectrum beginning from $P_{\text{in}} > 40$ mW and then causes a gradual "collapse" of the dipole gaps in the spin wave spectrum. This means that at a fixed frequency of the input carrier signal the parameters v_g and $\partial^2\omega/\partial k^2$ can vary rapidly if P_{in} is altered, particularly in the range $P_{\text{in}} > 40$ mW.

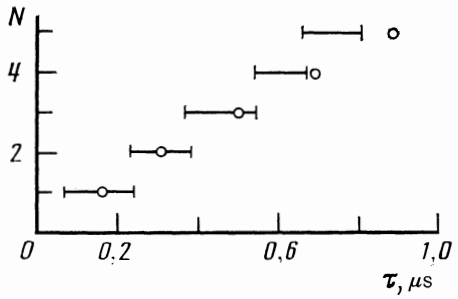

FIG. 9. Dependence of the number of solitons N on the duration τ of an input rectangular pulse: the segments are theoretical and the points are the experimental data.

Strong frequency dependences of the dispersion parameters v_g and $\partial^2\omega/\partial k^2$ explain, in our view, why just one (lowest) satellite is present in the spectrum of the signal transmitted by a ferromagnetic field (Figs. 6 and 8). It is clear from Fig. 8 that if the frequency of an input monochromatic signal is at the left-hand edge of a dipole gap in a strong dispersion region, then the spectral satellites formed as a result of the process described by Eq. (9) appear at different positions: the lower satellite is found in a zone characterized by $\partial^2\omega/\partial k^2 < 0$, whereas the upper satellite is in a zone $\partial^2\omega/\partial k^2 > 0$ and in the latter case the necessary condition for a parametric instability given by Eq. (14) is no longer obeyed. Moreover, the upper satellite is in a region with a lower group velocity and, consequently, stronger spatial attenuation.

However, it should be pointed out that experiments carried out under conditions of continuous excitation of magnetization waves in transversely magnetized YIG films have revealed effects which cannot be explained by the above model.

One of these effects is a modulational instability of magnetization waves observed when the amplitude of a monochromatic wave increased in those parts of the spectrum where $\partial^2\omega/\partial k^2 > 0$ and the Lighthill criterion of Eq. (13) is no longer obeyed (see Fig. 7 and also Refs. 9 and 26). This instability is characterized by a relatively small modulation depth and by a symmetric spectrum which contains both lower and upper satellites of comparable amplitudes.

It was shown in Ref. 9 and 10 that in the case of thin ferromagnetic films a very likely cause of such an instability is the parametric process of Eq. (9) when $\varkappa \sim k_0$. In this case the growth rate of four-magnon decay of Eq. (9) does not depend directly on the sign of the dispersion coefficient $\partial^2\omega/\partial k^2$ and the process can consequently be observed also where $\partial^2\omega/\partial k^2 > 0$. Another probable reason for self-modulation of a magnetization wave may be, in our opinion, the process of interaction of pairs of oppositely directed waves of Eq. (10), which in our experimental situation may be realized only near a transmitting antenna. In the case of bulk ferromagnets the process of Eq. (10) had been investigated before,[21,22,27] using the so-called S model and it was found that

the growth rate of this process did not depend directly on the sign of $\partial^2\omega/\partial k^2$.

The symmetric (independent of the sign and value of $\partial^2\omega/\partial k^2$) positions of satellites in the spectrum of the investigated instability [see Fig. 7 in the present paper, Fig. 1(2) in Ref. 9, and Fig. 1 in Ref. 26] and the reduction in the amplitude of the satellites away from the transmitting antenna[26] support the proposed explanation.

A second effect which cannot be explained on the basis of Eq. (11) is the transition from a coherent modulation regime to a stochastic one [see Figs. 6(7) and 6(8) in the present paper and Figs. 1(5) and 1(6) in Ref. 9], which occurs in the power of the input unmodulated signal. The effect is manifested particularly clearly in thin ($L < 1\ \mu$m) YIG films where high signal power densities can be achieved in the interior of a film.[9,10]

Several scenarios of the transition from a dynamic to a stochastic regime of parametric effects in ferromagnets have been suggested. A mechanism of secondary turbulence in a system of parametrically excited modulation waves is described in Refs. 22 and 28. Another possible mechanism of this transition to a stochastic regime is a kinetic instability[29] which is supported by the experimental results reported in Ref. 9. A recent experimental investigation of an obliquely magnetized YIG film[11] demonstrated a transition of a parametric instability of magnetization waves to a stochastic regime as a result of appearance of a strange attractor after a chain of different consecutive bifurcations.

Clearly, the relationships governing the transition to chaos in a system of magnetization waves cannot be established without more extensive experimental investigations.

6. CONCLUSIONS

The main result of the present study is the detection and determination of parameters of solitons representing envelopes of microwave magnetization waves generated under pulsed excitation conditions and a modulational instability of waves with the same frequency under conditions of continuous monochromatic excitation. It should be stressed particularly that the formation of envelope spin-wave solitons described above agrees with a physical definition of a soliton as an entity which exists because of an equilibrium between two competing factors, dispersion and nonlinearity.

Just above critical conditions the investigated nonlinear wave phenomena can be explained theoretically using the nonlinear Schrödinger equation. When the margin is relatively large, the propagation of nonlinear waves becomes very complicated and requires further study.

The great variety, relative simplicity of observation, and the existence of specific size characteristics of nonlinear wave phenomena discovered in recent years in epitaxial YIG films will ensure continuing attention of experimentalists and theoreticians.

[1)]Here and below all the values of the input microwave power are given after the signal reflected by the transmitting antenna is subtracted.

[2)]Similar noise modulation in YIG films was first pointed out in Ref. 9.

[3)]It should be pointed out that in the case of a tangentially magnetized film, where in contrast to a transversely magnetized film we have $\partial\omega/\partial|\varphi|^2 < 0$, the formation of envelope solitons is observed not at the left-hand edge of a dipole gap, but at the right-hand edge where $\partial^2\omega/\partial k^2 > 0$ (Ref. 15). This is an important argument in favor of the soliton mechanism of the observed effects.

[1]I. A. Akhiezer and A. E. Borovik, Zh. Eksp. Teor. Fiz. **52**, 508 (1967) [Sov. Phys. JETP **25**, 332 (1967)].
[2]E. B. Volzhan, N. P. Giorgadze, and A. D. Pataraya, Fiz. Tverd. Tela (Leningrad) **18**, 2546 (1976) [Sov. Phys. Solid State **18**, 1487 (1976)].
[3]A. M. Kosevich, B. A. Ivanov, and A. S. Kovalev, *Nonlinear Magnetization Waves: Dynamic and Topological Solitons* [in Russian], Naukova Dumka, Kiev (1983).
[4]A. V. Vashkovskiĭ, V. I. Zubkov, I. V. Krutsenko, and G. A. Melkov Pis'ma Zh. Eksp. Teor. Fiz. **39**, 124 (1984) [JETP Lett. **39**, 146 (1984)].
[5]V. S. Gornakov, L. M. Dedukh, and V. I. Nikitenko, Pis'ma Zh. Eksp. Teor. Fiz. **39**, 199 (1984) [JETP Lett. **39**, 236 (1984)].
[6]B. A. Kalinikos, N. G. Kovshikov, and A. N. Slavin, Pis'ma Zh. Eksp. Teor. Fiz. **38**, 343 (1983) [JETP Lett. **38**, 413 (1983)].
[7]B. A. Kalinikos, N. G. Kovshikov, and A. N. Slavin, Fiz. Tverd. Tela (Leningrad) **27**, 226 (1985) [Sov. Phys. Solid State **27**, 138 (1985)].
[8]B. A. Kalinikos, N. G. Kovshikov, and A. N. Slavin, Pis'ma Zh. Tekh. Fiz. **10**, 936 (1984) [Sov. Tech. Phys. Lett. **10**, 392 (1984)].
[9]P. E. Zil'berman, S. A. Nikitov, and A. G. Temiryazev, Pis'ma Zh. Eksp. Teor. Fiz. **42**, 92 (1985) [JETP Lett. **42**, 110 (1985)].
[10]Yu. V. Gulyaev, P. E. Zil'berman, S. A. Nikitov, and A. G. Temiryazev, Fiz. Tverd. Tela (Leningrad) **28**, 2774 (1986) [Sov. Phys. Solid State **28**, 1553 (1986)].
[11]G. M. Dudko, G. T. Kazakov, A. V. Kozhevnikov, and Yu. A. Filimonov, Pis'ma Zh. Tekh. Fiz. **13**, 736 (1987) [Sov. Tech. Phys. Lett. **13**, 306 (1987)].
[12]B. A. Kalinikos, Izv. Vyssh. Uchebn. Zaved. Fiz. No. 8, 42 (1981).
[13]B. A. Kalinikos and A. N. Slavin J. Phys. C **19**, 7013 (1986).
[14]V. F. Dmitriev, B. A. Kalinikos, and N. G. Kovshikov, Zh. Tekh. Fiz. **55**, 2051 (1985) [Sov. Phys. Tech. Phys. **30**, 1206 (1985)].
[15]B. A. Kalinikos and A. N. Slavin, Fiz. Tverd. Tela (Leningrad) **26**, 3456 (1984) [Sov. Phys. Solid State **26**, 2077 (1984)].
[16]V. I. Karpman, *Nonlinear Waves in Dispersive Media* [in Russian], Nauka, Moscow (1973), p. 133.
[17]V. P. Lukomskiĭ, Ukr. Fiz. Zh. **23**, 134 (1978).
[18]A. K. Zvezdin and A. F. Popkov, Zh. Eksp. Teor. Fiz. **84**, 606 (1983) [Sov. Phys. JETP **57**, 350 (1983)].
[19]A. N. Slavin and B. A. Kalinikos, Zh. Tekh. Fiz. **57**, 2387 (1987) [Sov. Phys. Tech. Phys. (to be published)].
[20]V. E. Zakharov, Zh. Prikl. Mekh. Tekh. Fiz. No. 2, 86 (1968).
[21]V. E. Zakharov, V. S. L'vov, and S. S. Starobinets, Usp. Fiz. Nauk **114**, 609 (1974) [Sov. Phys. Usp. **17**, 896 (1975)].
[22]V. S. L'vov, A. M. Rubenchik, V. V. Sobolev, and V. S. Synakh, Fiz. Tverd. Tela (Leningrad) **15**, 793 (1973) [Sov. Phys. Solid State **15**, 550 (1973)].
[23]V. E. Zakharov, S. V. Manakov, S. P. Novikov, and L. P. Pitaevskiĭ, *Theory of Solitons: Inverse Problem Method* [in Russian], Nauka, Moscow (1980).
[24]V. E. Zakharov, V. S. L'vov, and S. S. Starobinets, Fiz. Tverd. Tela (Leningrad) **11**, 2922 (1969) [Sov. Phys. Solid State **11**, 2368 (1970)].
[25]A. L. Fabrikant, Zh. Eksp. Teor. Fiz. **84**, 470 (1984) [Sov. Phys. JETP **59**, 274 (1984)].
[26]P. E. Zil'berman, G. T. Kazakov, and V. V. Tikhonov, Pis'ma Zh. Tekh. Fiz. **11**, 769 (1985) [Sov. Tech. Phys. Lett. **11**, 319 (1985)].
[27]V. S. L'vov, Fiz. Tverd. Tela (Leningrad) **13**, 3488 (1971) [Sov. Phys. Solid State **13**, 2949 (1972)].
[28]V. L. Grankin, V. S. L'vov, V. I. Motorin, and S. L. Musher, Zh. Eksp. Teor. Fiz. **81**, 757 (1981) [Sov. Phys. JETP **54**, 405 (1981)].
[29]A. V. Lavrinenko, V. S. L'vov, G. A. Melkov, and V. B. Cherepanov, Zh. Eksp. Teor. Fiz. **81**, 1022 (1981) [Sov. Phys. JETP **54**, 542 (1981)].

Translated by A. Tybulewicz